J Appl Electrochem (2010) 40:2005–2012
DOI 10.1007/s10800-010-0180-0

ORIGINAL PAPER

Studies on the electrochemical reduction processes of $HTeO_2^+$ by CV and EIS

Fei-Hui Li · Wei Wang

Received: 29 November 2009 / Accepted: 18 July 2010 / Published online: 31 July 2010

Abstract Electrochemical characterizations of the underpotential deposition of tellurium on Au substrate were investigated by cyclic voltammetry (CV) in this paper. The results showed that the irreversible underpotential deposition of Te could take place once the Au electrode was immersed into the $HTeO_2^+$ solution. The redox behaviors of adsorbed $HTeO_2^+$ were also studied and the results revealed that $HTeO_2^+$ could only adsorb on Au electrode surface. The kinetics relating to the reduction of adsorbed $HTeO_2^+$ could be affected by $HTeO_2^+$ concentration but the charge consumed by the reduction of adsorbed $HTeO_2^+$ was concentration-independent. Electrochemical impedance spectroscopy (EIS) analyses about the bulk formation process of Te^0 indicated that during the bulk reduction of $HTeO_2^+$ to Te^0, four electrons were not obtained simultaneously in only one electrochemical step, some intermediate products, which need to be further detected and investigated in the future researches, might emerged in the intermediate processes.

Keywords Electrochemical · $HTeO_2^+$ · Underpotential deposition · Adsorption

1 Introduction

Bismuth telluride and its derivative compounds are considered to be the best suitable thermoelectric materials used to fabricate thermoelectric devices near room temperature. The fabricating technologies for bismuth telluride and its derivative compounds thin film also attract wide attentions recently for their usage in the manufacture of micro-thermoelectric devices, such as micro-cooler, micro-generator and so on. Those micro-thermoelectric components are very important in the fields such as micro-electro-mechanical systems (MEMS) and microelectronics. Physical methods and chemical methods are used to fabricate film thermoelectric materials, mainly including physical vapour deposition (PVD) [1], metal organic chemical vapor deposition (MOCVD) [2], electrodepositon [3] technology and so on. The remarkable advantages of electrodepositon [4] are its low cost, easy operation and suitable for large scale production. Moreover, the doping concentration and crystalline state of the electrodeposited thermoelectric films can be easily controlled by adjusting the electrodepositing parameters and the composition of the electrolyte.

Despite that there are large amount of literatures researching the preparation of bismuth telluride based film materials using electrochemical techniques [5–11], only a few of literatures refer to the electrochemical reduction process [12–17] which has great effects on the preparation of the materials using electrodeposition techniques, and most of them only focus on the underpotential deposition (UPD) process [13–15]. But in fact, the adsorptive behavior of the ions as well as the bulk formation process also plays an important role in the electrodeposition of bismuth telluride based compound. Thinking of this, some basic researches have been done in our lab aiming at exploring the electrochemical reduction process of $HTeO_2^+$ to Te^0 on Au electrode surface.

In this paper, the electrochemical behaviors of Te UPD, the electrochemical behaviors of adsorbed $HTeO_2^+$ as well as the electrochemical behaviors of Te bulk formation are all investigated on Au electrode using cyclic voltammetry

F.-H. Li · W. Wang (✉)
Department of Applied Chemistry, School of Chemical Engineering and Technology, Tianjin University, Tianjin 300072, People's Republic of China
e-mail: wwtju@yahoo.cn

(CV) and electrochemical impedance spectroscopy (EIS) measurements, and some new conclusions and useful information concerning the reduction process of $HTeO_2^+$ to Te^0 are obtained.

2 Experimental section

2.1 Solution

All chemicals were analytical grade without special explanation and the electrolytes were prepared with redistilled water to ensure the stabilities of ions in the solutions. The Te^{IV} nitric acid solutions (pH $\approx$ 0.66) was prepared by dissolution of H_2TeO_3 (chemical pure) in concentrated HNO_3 aqueous solution, followed by diluting the HNO_3 to 1 M. The existence form of Te^{IV} in acidic solution (pH = 0–1) was generally considered to be $HTeO_2^+$ [18].

2.2 Electrochemical measurement

All the electrochemical measurements were performed using CHI660B electrochemical working station (manufactured by Shanghai Chenhua Apparatus Company) at 25 ± 1 °C. A standard three-electrode cell was used for the electrochemical measurement, which consisted of a polycrystalline Au plate (1 cm^2) as the working electrode, a Pt plate as the auxiliary electrode and a saturated calomel electrode (SCE) as the reference electrode. The working electrode was mechanical polished, electrochemical degreased, etched in concentrated HNO_3 solution and rinsed with redistilled water in order to ensure a clean surface before the measurements. All the potentials were measured and expressed related to the aqueous KCl SCE. Solutions were not stirred during all the electrochemical measurements. Solutions were deoxygenated by passing dry nitrogen through the solution prior to each experiment. The cyclic voltammograms were recorded at different scanning rates. The EIS measurements were carried out in the frequency range of 1 mHz to 100 kHz at different polarizing potentials, and the applied potentials amplitude was 5 mV.

3 Results and discussion

3.1 Electrochemical behaviors of Te UPD on Au electrode

The electrochemical reduction of $HTeO_2^+$ to Te^0 can be described by Eq. 1 [19]. According to Nernst Equation, the equilibrium electrode potential $\varphi_e(HTeO_2^+/Te^0)$ of Eq. 1 can be written as Eq. 2 at 25 °C, where $\varphi^\theta(HTeO_2^+/Te^0)$ is the standard electrode potential equaling 0.551 V versus a saturated hydrogen electrode (SHE), and $a(HTeO_2^+)$, $a(H^+)$, $a(H_2O)$ and $a(Te^0)$ are the activities of $HTeO_2^+$, H^+, H_2O and Te^0, respectively.

$$\begin{aligned} &HTeO_2^+ + 4e^- + 3H^+ \rightarrow Te^0 + 2H_2O \\ &\varphi^\theta_{(HTeO_2^+/Te^0)} = 0.551\,\text{V vs. SHE} \end{aligned} \quad (1)$$

$$\begin{aligned} \varphi_{e(HTeO_2^+/Te^0)} &= \varphi^\theta_{(HTeO_2^+/Te^0)} + \frac{RT}{nF}\ln\frac{a(HTeO_2^+)\cdot a^3(H^+)}{a(Te^0)\cdot a^2(H_2O)} \\ &= \varphi^\theta_{(HTeO_2^+/Te^0)} + \frac{0.05916}{4}\lg\frac{a(HTeO_2^+)\cdot a^3(H^+)}{a(Te^0)\cdot a^2(H_2O)} \\ &= \varphi^\theta_{(HTeO_2^+/Te^0)} + 0.01479\lg\frac{a(HTeO_2^+)}{a(Te^0)\cdot a^2(H_2O)} \\ &\quad - 0.04437\,\text{pH} \end{aligned} \quad (2)$$

It is well known that ion activity is close to its molar concentration in diluted solutions. So $\varphi_{e(HTeO_2^+/Te^0)}$ can be calculated to be 0.4877 versus SHE (equals to 0.2467 V vs. SCE) according Eq. 2 by substituting $a(HTeO_2^+)$, $a(H_2O)$, $a(Te^0)$ and pH with 0.005 M, 1, 1 and 0.66, respectively.

Figure 1 shows the cyclic voltammogram of Au electrode in the solution containing 5 mM $HTeO_2^+$ and 1 M HNO_3. The cathodic scanning was started at 0.4 V and four reductive peaks (labeled A–D) can be observed in the cathodic branch of the second cycle in Fig. 1. In the positive branch, the cyclic voltammogram shows two oxidation peaks (labeled E, F), which should correspond to the anodic stripping of Te^0. By comparing the reduction peak potentials of the four reduction peaks with $\varphi_{e(HTeO_2^+/Te^0)}$, it can be found that only the peak potential of peak A is positive than $\varphi_{e(HTeO_2^+/Te^0)}$ while those of the peak B ~ D are all negative than $\varphi_{e(HTeO_2^+/Te^0)}$. It reveals that the reductive process

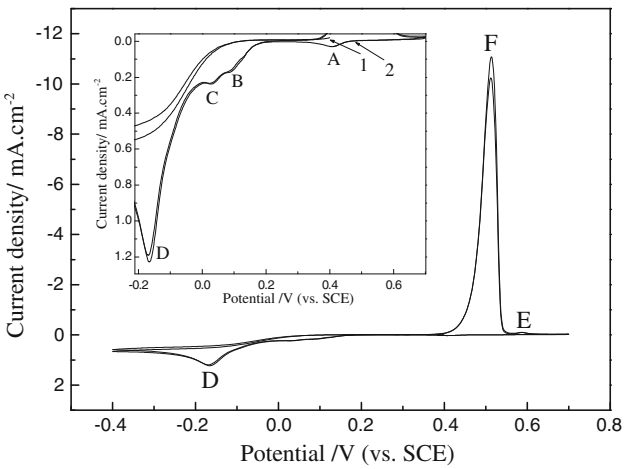

Fig. 1 Cyclic voltammogram of Au electrode in the solution containing 5 mM $HTeO_2^+$ and 1 M HNO_3. The numeral indicates consecutive scans, scanning rate: 10 mV/s

corresponding to peak A is the UPD of $HTeO_2^+$. Similar results can also be gained on Au(111) in other acid systems, like H_2SO_4 and $HClO_4$ [13, 14], which also shows that a UPD feature can be firstly observed in the reduction process of $HTeO_2^+$. According to the CV images in Fig. 1, the charge consumed by the Te UPD can be calculated to be 284.3μC/cm^2 (the charge consumed by 1 M HNO_3 blank electrolyte had been subtracted from the total charge amount), which corresponds to the coverage of 0.32 (defined as ratio of the number of Te atoms to that of Au atoms on the electrode surface) on the polycrystalline Au electrode surface. This charge agrees well with that gained from STM study of the UPD Te on Au(111) by Stickney and co-workers [14]. What can also be found from Fig. 1 is that the UPD peak A can only be observed in the second scanning cycle of the CV, and its appearing has no effect on the shape of the following reduction peaks.

In order to gain more information about the redox process corresponding to peak A, multi-cycle CV measurement were performed in the potential range of 0.25–0.7 V. It can be seen that the cyclic voltammogram shows one redox couple (reduction peak A and oxidation peak E) in the scanning potential range. Since peak A has been confirmed to be the UPD of Te^0, the oxidation peak E appearing at around 0.6 V should correspond to the anodic stripping of UPD Te^0. It is well known that the peak separation ($\Delta\varphi_p$) between the oxidation peak and reduction peak can be used as a powerful criterion in judging the reversibility of a redox process. [20] So $\Delta\varphi_{p1}$ between the peak A and peak E was calculated and a value ($\Delta\varphi_{p1} = \varphi_{pa1} - \varphi_{pc1} = 179$ mV) much higher than $2.3RT/nF$ (equals to 14.75 mV after substitute R, T, n, F with 8.314 J K^{-1} mol^{-1}, 298.15 K, 4 and 96500 °C mol^{-1}) was gained. This result means that the Te UPD and stripping on Au electrode surface is an irreversible process. What can also be found in Fig. 2 is that when the potential scans back without passing the oxidation peak E, no reduction peak can be observed in the reverse scanning, vice versa, when the potential scans back without passing the reduction peak A, no oxidation peak can be observed in the reverse scanning. The former phenomenon can be explained by the following reason: UPD of $HTeO_2^+$ to Te^0 can only occur on naked Au electrode surface, once the UPD takes place, the naked Au electrode surface will be covered by UPD Te^0, so the UPD can not be performed unless the Te^0 covered on the naked Au electrode surface is stripped during the oxidation process. The latter phenomenon is due to that no Te^0 is produced if the potential scans back without passing the reduction peak, accordingly, no oxidation peak relates to the oxidation of Te^0 to $HTeO_2^+$ will appear. Moreover, another interesting phenomenon can also be found in Fig. 2. In the first cycle of the cyclic voltammogram, the potential scanning was started at open circuit potential (0.281 V vs. SCE) towards positive direction, although no reduction process was carried out

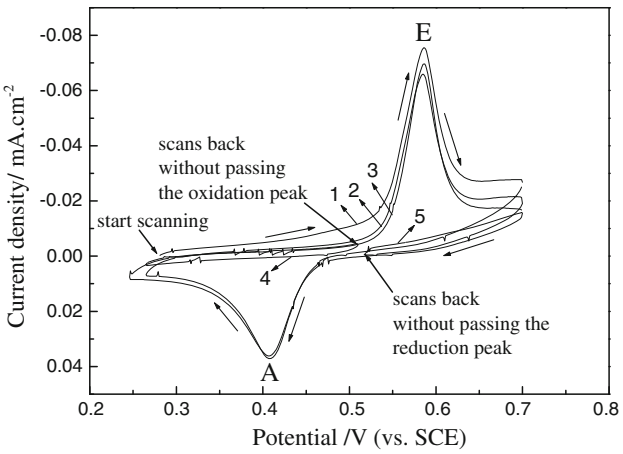

Fig. 2 Multi-cycle cyclic voltammogram of Te UPD on Au electrode in the solution containing 5 mM $HTeO_2^+$ and 1 M HNO_3. The numeral indicates consecutive scans, scanning rate: 10 mV/s

before the anodic scanning, peak E, which corresponds to the oxidation of UPD Te^0 to $HTeO_2^+$, can still be observed. So it can be conjectured that Te UPD can arise once the Au electrode is immersed into the $HTeO_2^+$ solution. In order to verify this conjecture, the following experiment was performed.

A clean Au electrode was firstly immersed into 5 mM $HTeO_2^+$ nitric acid solution for 2 min, and then rinsed with 1 M HNO_3 blank aqueous solution adequately to avoid bringing dissociative $HTeO_2^+$ into the solution in the sequential CV measurement. After that, multi-cycle CV measurement was performed on this Au electrode in 1 M HNO_3 blank aqueous solution. Corresponding result is shown in Fig. 3b). Comparing the cyclic voltammogram

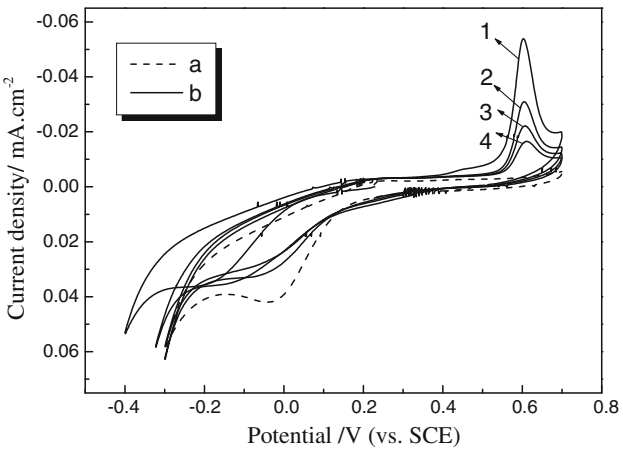

Fig. 3 Cyclic voltammograms of Au electrode covered with UPD Te^0 in 1 M HNO_3 solution (*solid line*) and clean Au electrode in 1 M HNO_3 solution (*dash line*), the numeral indicates consecutive scans, scanning rate: 10 mV/s

measured on a clean Au electrode in 1 M HNO_3 solution (Fig. 3a with curve b), it can be found that both curves a and b show a wide reduction peak, which may be caused by the reduction of NO_3^- in the solution, in the cathodic branches, while an obvious oxidation peak (at around 0.6 V) with the peak potential closing to the oxidation potential of UPD Te^0 can only be observed in the anodic branch in curve b). These results clearly reveal that UPD Te^0 is formed during the immersing of Au electrode in the $HTeO_2^+$ nitric acid solution, which means that the UPD of tellurium can take place under open circuit potential. And these analyses can well explain why UPD peak A can not be observed in the first cycle of cyclic voltammogram in Fig. 1. Curve b also show that the intensity of the oxidation peak decrease with the increase of the cycle number, it is due to that the UPD Te^0 is oxided to $HTeO_2^+$ and diffuses into the solution in the anodic scanning, less UPD Te^0 will be formed in the next reverse scanning, and leads to the intensity decrease of the oxidation peak in the following scanning cycle.

The effect of $HTeO_2^+$ concentration on the Te UPD process was investigated using CV measurement. Figure 4 shows the cyclic voltammograms measured on Au electrode in the solutions containing 1 M HNO_3 and different concentrations of $HTeO_2^+$. From integration of the current densities of peak A, it can be found that the charge consumed by peak A are practically coincident in spite of the change of the ion concentration. Since UPD is a surface-limited process, the charge consumed by the UPD is independent of ion concentration. From Fig. 4, it can also be noticed that decreasing of $HTeO_2^+$ concentration arises a negative shift of the reduction peak A. It indicates that the UPD of $HTeO_2^+$ to Te^0 becomes difficult with the decreasing of $HTeO_2^+$ concentration, which should be attributed to the decreasing of mass transport rate of ion to electrode surface in the solution with lower ion concentration. Similar results can also be gained on Au(111) in $HClO_4$ systems [13].

3.2 Electrochemical behavior of adsorbed $HTeO_2^+$ on Au electrode

Figure 1 shows that four reduction peaks (peak A–D) corresponding to the reduction of $HTeO_2^+$ on Au electrode can be observed in the cathodic process. Peak A, which is attributed to the UPD of Te, has been analyzed in detail in Sect. 3.1. In order to get more information about the reduction process corresponding to the other three reduction peaks, the CV images of Au electrode in 0.005 mol/L $HTeO_2^+$ acidic solution were measured under different scanning rates (shown in Fig. 5).

It is well known that the peak current density i_p in cyclic voltammogram will change with the potential scanning rate υ. According to Langmuir [21] isothermal adsorption rule, there is a linear relationship (shown in Eq. 3) between i_p and υ if ion adsorption exists in the corresponding irreversible reaction:

$$i_p = \frac{\alpha F^2 A \upsilon \Gamma^*}{2.718RT} \tag{3}$$

while i_p will change linearly with the extracting roots of scanning rate $\upsilon^{1/2}$ (according to Eq. 4) if the current peak is caused by ion diffusion [22] in the corresponding irreversible reaction:

$$i_p = (2.99 \times 10^5)\alpha^{1/2} A D_0^{1/2} C_0^* \upsilon^{1/2} \tag{4}$$

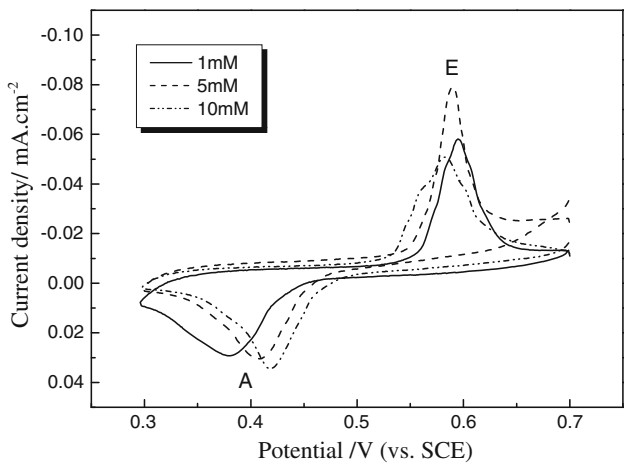

Fig. 4 Cyclic voltammograms of Au electrode in the solutions containing 1 M HNO_3 and different concentrations of $HTeO_2^+$. *Solid line* 1 mM $HTeO_2^+$, *dash line* 5 mM $HTeO_2^+$, *dash dot line* 10 mM $HTeO_2^+$, scanning rates: 10 mV/s

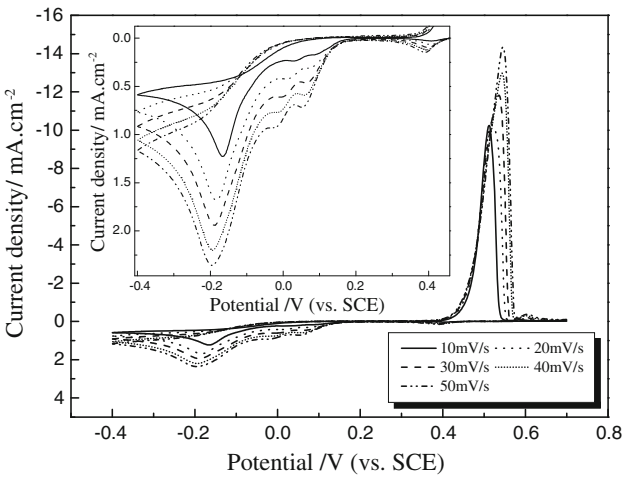

Fig. 5 Cyclic voltammograms of Au electrode in the solution containing 5 mM $HTeO_2^+$ and 1 M HNO_3 at different scanning rates, scanning rates are 10, 20, 30, 40 and 50 mV/s, separately. *Inset* partly amplified CVs

where n is the number of electrons transferring in the electrochemical reaction, F is the Faraday constant, R is the gas constant, T is the temperature, α is the transport coefficient, Γ^* is the surface excess of adsorptive particles on the electrode surface when $t = 0$, A is the electrode area, C_0^* is the bulk concentration of the reactant in the solution, D_0 is the diffusion coefficient, and υ is the potential scanning rate.

The i_p value of peak B–D under different scanning rates can be obtained from Fig. 5. The relationships between i_p and υ as well as i_p and $\upsilon^{1/2}$ for peaks B–D are shown in Fig. 6 by black hollow and red solid points separately, while the black dash and red solid lines in Fig. 6 are their corresponding linear fitting regression lines. It can be seen from Fig. 6 that there is a very good linear relationship between i_p and υ for peak B, peak C and between i_p and $\upsilon^{1/2}$ for peak D. This reveals that adsorptive phenomena exist in the cathodic reduction processes corresponding to peak B and peak C, while peak D is caused only by the ion diffusion. So peak B and peak C can be conjectured as representing the reduction of adsorbed $HTeO_2^+$ while peak D is the bulk deposition of dissociative $HTeO_2^+$.

The effect of $HTeO_2^+$ concentration on the redox behavior of adsorbed $HTeO_2^+$ was also investigated using CV measurement and corresponding results are shown in Fig. 7. It can be seen when the potential scans back after passing the reduction peak B and peak C, a sharp oxidation peak (labeled G) appears at 0.438 V in the anodic scanning process. This suggests that peak G is the anodic stripping of Te^0 reduced by adsorbed $HTeO_2^+$. The obvious difference in peak potentials and peak shapes between the reduction

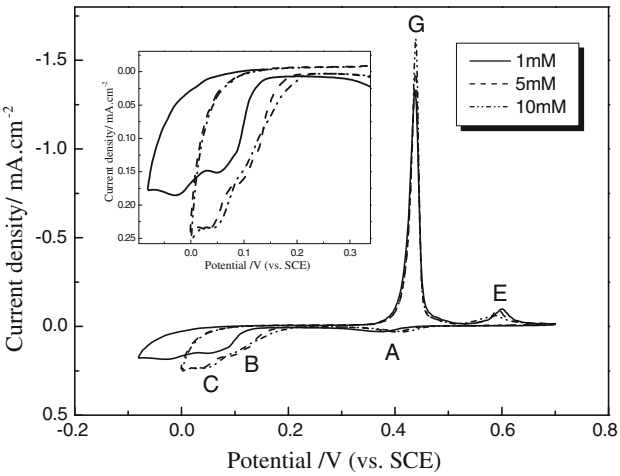

Fig. 7 Cyclic voltammograms of Au electrode in the solutions containing 1 M HNO_3 and different concentrations of $HTeO_2^+$. *Solid line* 1 mM $HTeO_2^+$, *dash line* 5 mM $HTeO_2^+$, *dash dot line* 10 mM $HTeO_2^+$, scanning rates: 10 mV/s

Fig. 6 Relationships between i_p and υ (*black hollow points* and *black dash line*) as well as i_p and $\upsilon^{1/2}$ (*red solid points* and *red solid line*) for peak *B*, peak *C* and peak *D* in Fig. 5. **a** Peak *B*, **b** peak *C*, **c** peak *D*. *Points* measured data; *lines* linear fitting regression results

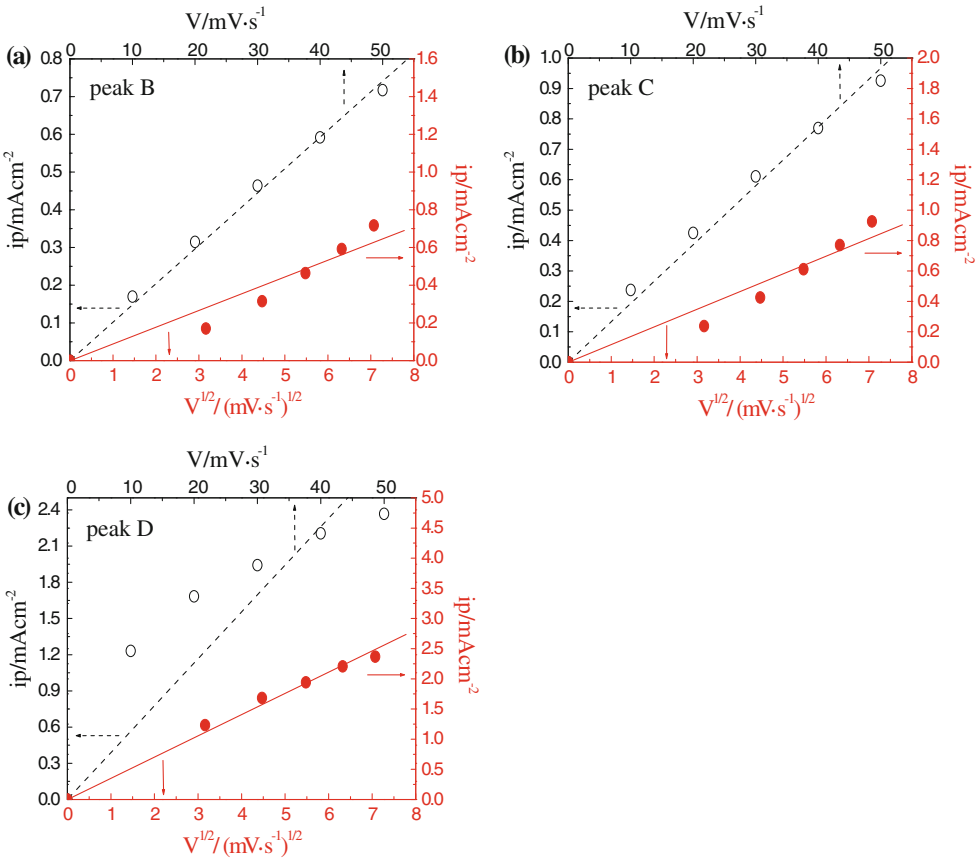

peaks and oxidation peak reveals that the redox of adsorbed $HTeO_2^+/Te^0$ is an irreversible process on the Au electrode surface. It can also be noticed that peak G shows a concentration-independent feature. From integration of the current densities of peak G, it can be found that charge consumed by peak G is practically coincident in spite of the change of ion concentration. This phenomenon further confirmed that peak B and peak C are corresponding to the reduction of adsorbed $HTeO_2^+$, which is a surface-limited process and thus is independent of the ion concentration. In contrast to the concentration-independent feature of peak G, reduction peak B and peak C show a negative shift with the decreasing of the $HTeO_2^+$ concentration. This suggests that the reduction of adsorbed $HTeO_2^+$ becomes sluggish in the solution with lower $HTeO_2^+$ concentration, which is due to the kinetic complications in solutions with lower $HTeO_2^+$ concentration.

Another conclusion concerning the adsorptive behavior of $HTeO_2^+$ can be gained from the cyclic voltammogram in Fig. 3b), which has been analyzed previously from other aspects in Sect. 3.1. It has been mentioned in Sect. 3.1 that before this CV measurement in 1 M HNO_3 blank aqueous solution, a clean Au electrode was firstly immersed into 5 mM $HTeO_2^+$ nitric acid solution for 2 min, and then rinsed with 1 M HNO_3 blank aqueous solution adequately. It can be obviously noticed that no redox peak corresponding to the adsorbed $HTeO_2^+/Te^0$ (reduction peak B, peak C and oxidation peak G) appears in the cyclic voltammogram in Fig. 3b). This result means that the adsorption of $HTeO_2^+$ on Au electrode surface is not very strong and the adsorbed $HTeO_2^+$ will desorb from the Au electrode surface during rinsing. This conclusion is contrary to the illustration reported by Zhu's group, [13] which refer that when the Au electrode is in contact with the $HTeO_2^+$ solution, $HTeO_2^+$ will strongly adsorb on the electrode and the interaction is so strong or irreversible that the adsorbed Te species remains on the surfaces even during rinsing.

Moreover, the adsorptive behavior of $HTeO_2^+$ on different substrate was also investigated using CV measurement. Figure 8 show a multi-cycle cyclic voltammogram of Au electrode covered with a layer of deposited Te^0 in the solution containing 5 mM $HTeO_2^+$ and 1 M HNO_3. Before the CV measurement, a static polarizing potential (−0.2 V vs. SCE) was applied on the Au electrode for 10 s, after that, a thin layer of Te^0 with silvery luster was deposited and covered on the Au electrode surface. From Fig. 8, it can be seen that only the reduction peak D, which corresponds to the bulk reduction of dissociative $HTeO_2^+$, can be observed in the cathodic branch in the first cycle of the cyclic voltammogram, after completing the oxidation in the reverse scanning, reduction peak B and peak C, which correspond to the reduction of adsorbed $HTeO_2^+$, appears

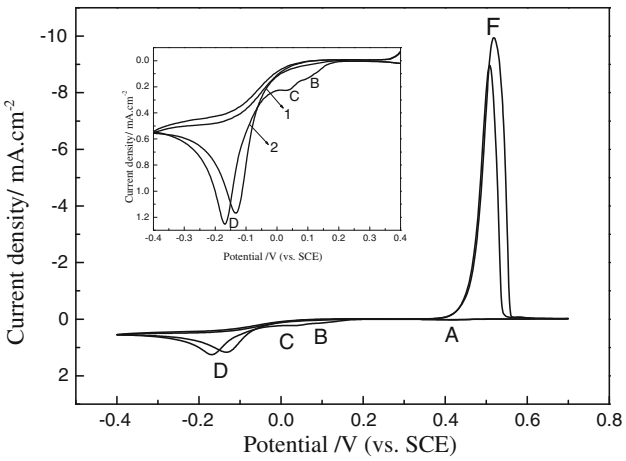

Fig. 8 Multi-cycle cyclic voltammogram of Au electrode covered with a layer of deposited Te^0 in the solution containing 5 mM $HTeO_2^+$ and 1 M HNO_3, the numeral indicates consecutive scans, scanning rates: 10 mV/s. *Inset* partly amplified CVs

in the following cathodic scanning process (the second cycle of cyclic voltammogram). These results indicate that the adsorption of $HTeO_2^+$ can only take place on Au electrode surface. In the cathodic scanning of the first cycle, the CV measurement is conducted on the Te substrate, since $HTeO_2^+$ can not be adsorbed on the Te substrate, peak B and peak C can not be seen in the cyclic voltammogram. After the reverse anodic scanning, the predeposited Te layer is oxided completely and naked Au electrode surface, as a result, comes out, which means that the cathodic scanning in the second cycle is performed on Au substrate. Since $HTeO_2^+$ adsorption can take place on Au electrode surface, peak B and peak C appears in the second cycle of the cyclic voltammogram.

3.3 Electrochemical behavior of Te bulk formation on Au electrode

The analyses in Sect. 3.1 and 3.2 have revealed that the reduction peak D in Fig. 1 corresponds to the bulk formation of Te^0 while the oxidation peak F located at 0.513 V relates to its anodic stripping. The obvious differences in peak potentials and peak shapes between the reduction peak D and oxidation peak F reveal that the bulk formation of Te^0 and its anodic stripping is an irreversible process on the Au electrode surface.

In order to get more information about the bulk formation process of Te^0, EIS measurements were performed at different potentials chose in the potential range of peak D and the corresponding Nyquist and Bode plots are shown in Fig. 9.

It can be seen that the Nyquist plots measured at potential 10 mV is comprised of a large semi-circle in high frequency region and a small semi-circle in low frequency

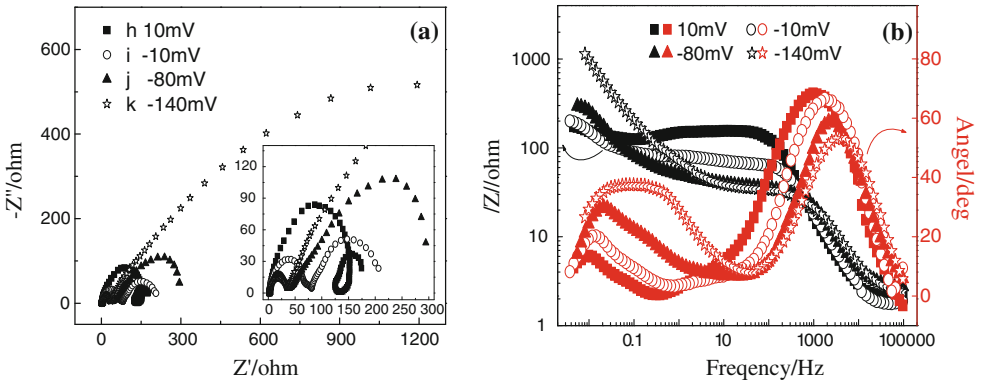

Fig. 9 EIS plots measured at different potentials in 10 mM $HTeO_2^+$ acidic solution on Au electrode. **a** are Nyquist plots; **a′** are Bode plots

region, which means that two electrochemical reactions take place at this potential. As the potential moving negatively, the small semi-circle in low frequency region becomes smaller and finally disappears at −80 mV, while a new semicircle in low frequency region appears at −10 mV. The new semicircle becomes larger gradually as the potential moving negatively and its shape finally close to a line with a slope closing to 1 at −110 mV. This result reveals that the new semicircle is caused by the finite diffusion of the reactant, and the finite diffusion will slowly change to semi-infinite diffusion with the overpotential increasing. Comparing the diameter of the two potential-dependent semicircles associated with the electrochemical reaction, it could be found that the diameter of the semicircle in lower frequency range is much smaller than that in higher frequency range. It indicates that the electrochemical reaction in lower frequency range is much easier than that in higher frequency range and is the rate-controlling step.

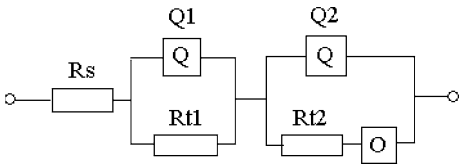

Fig. 10 Equivalent circuit using to model the EIS plot measured at potential −10 mV

In order to further prove that the later-appeared semicircle is caused by the finite diffusion of the reactant instead of representing a electrochemical reaction, the Nyquist and Bode plots measured at potential −10 mV was simulated using an equivalent circuit shown in Fig. 10, where R_s is the uncompensated solution resistance from the reference electrode to the working electrode, Q is the constant phase element, R_t is the resistance of the charge transfer at the electrode–electrolyte interface, O represents the resistance of finite diffusion on plane electrode.

Figure 11 shows the Nyquist and Bode plots measured at −10 mV and their simulated results using the equivalent circuit in Fig. 10. It can be found that the simulated curve is consistent very well with the measured data, which indicated that the equivalent circuit shown in Fig. 10 is suitable to describe the electrochemical reaction process. The results also prove that the later-appearing semicircle in the Nyquist plots is indeed caused by the finite diffusion of the reactant ion.

The EIS analyses above indicates that the reduction of $HTeO_2^+$ to Te^0 is not completed through only one electrochemical step, which means that during the reduction of $HTeO_2^+$ to Te^0, the four electrons are not obtained simultaneously in only one electrochemical step, some

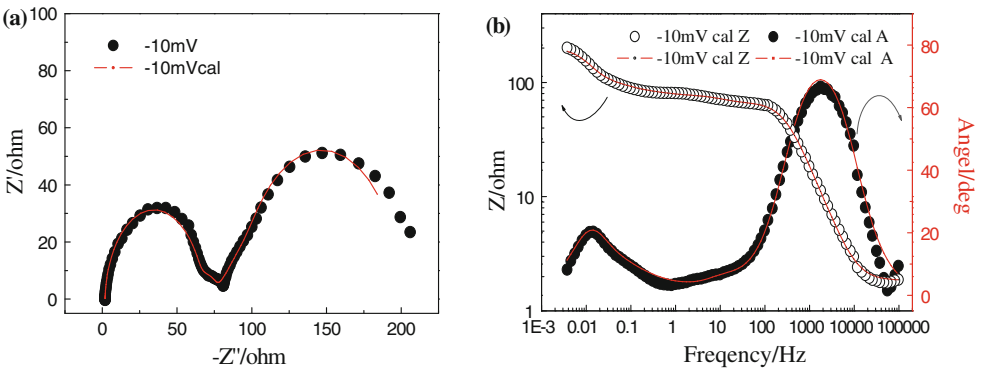

Fig. 11 Nyquist (**a**) and Bode (**b**) plots measured at −10 mV and their simulated results according to the equivalent circuit in Fig. 10

intermediate products, which need to be further detected and investigated in the future researches, may emerged in the intermediate processes. This result is consistent with the electrochemical principles [23], which mention that it is possible to obtain one or two electrons in one electrochemical step, but it is almost impossible to obtain more than three electrons only in one-step electrochemical reaction. But in many literatures, this point is neglected and the deposition process of $HTeO_2^+$ is considered as completed by a four-electron reduction step [24–27]: $HTeO_2^+ + 4e^- + 3H^+ \rightarrow Te^0 + 2H_2O$

4 Conclusion

The Te UPD, the adsorptive behaviors of $HTeO_2^+$ as well as the bulk formation of Te^0 were investigated using CV and EIS measurements. The results show that the UPD of Te is an irreversible process and can take place once the Au electrode is immersed into the $HTeO_2^+$ solution, the UPD process kinetics is sensitive to the $HTeO_2^+$ concentration but the charge consumed by the UPD is concentration-independent. Researches on the adsorptive behaviors of $HTeO_2^+$ ion reveal that $HTeO_2^+$ can only adsorb on Au electrode surface, but the interaction between the adsorbed $HTeO_2^+$ and Au electrode surface is not very strong since the adsorbed $HTeO_2^+$ ion can desorb from the Au electrode surface during rinsing. The kinetics relating to the reduction of adsorbed $HTeO_2^+$ can be affected by $HTeO_2^+$ concentration but the charge consumed by the reduction of adsorbed $HTeO_2^+$ is concentration-independent. EIS analyses about the bulk formation of Te^0 indicates that during the bulk reduction of $HTeO_2^+$ to Te^0, the four electrons are not obtained simultaneously in only one electrochemical step, some intermediate products, which need to be further detected and investigated in the future researches, may emerged in the intermediate processes.

Acknowledgments This work is co-supported by International Cooperation Project of Chinese Science and Technology Ministry (2009DFA62700) and Doctorial Fundation Project of Chinese Education Ministry (200800560002).

References

1. Kim IH (2000) Mater Lett 44:75
2. Venkatasubramanian R, Colpitts T, Watko E, Lamvik M, El-Masry N (1997) J Cryst Growth 170:817
3. Yoo BY, Huangb C-K, Limb JR, Hermanb J, Ryanb MA, Fleurial J-P, Myung NV (2005) Electrochim Acta 50:4371
4. Miyazaki Y, Kajitani TJ (2001) Cryst Growth 229:542
5. Ebe H, Ueda M, Ohtsuka T (2007) Electrochim Acta 53:100
6. Xing-Hua Li, Zhou B, Pu L, Zhu J-J (2008) Cryst Growth Des 8:771
7. Frari DD, Diliberto S, Stein N, Boulanger C, Lecuire JM (2006) J Appl Electrochem 36:449
8. Bu L, Wang W, Wang H (2007) Appl Surf Sci 253:3360
9. Martín-González MS, Priet AL, Gronsky R, Sands T, Stacy AM (2002) J Electrochem Soc 149:C546
10. Xiao F, Hangarter C, Yoo B, Rheem Y, Lee K-H, Myung NV (2008) Electrochim Acta 53:8103
11. Menke EJ, Brown MA, Li Q, Hemminger JC, Penner RM (2006) Langmuir 22:10564
12. Li WS, Long XM, Yan JH, Nan JM, Chen HY, Wu YM (2006) J Power Sources 158:1096
13. Zhu W, Yang JY, Zhou DX, Bao SQ, Fan XA, Duan XK (2007) Electrochim Acta 52:3660
14. Sorenson TA, Varazo K, Wayne Suggs D, Stickney JL (2001) Surf Sci 470:197
15. Yagi I, Lantz JM, Nakabayashi S, Corn RM, Uosaki K (1996) J Electroanal Chem 401:95
16. Jung C, Rhee CK (2005) J Phys Chem B 109:8961
17. Hara M, Inukai J, Yoshimoto S, Itaya K (2004) J Phys Chem B 108:17441
18. Murase K, Watanabe H, Hirato T, Awakura Y (1999) J Electrochem Soc 146:1798
19. Møller C, Plesset MS (1934) Phys Rev 46:618
20. Bard AJ, Faulkner LR (2005) Electrochemical methods fundamentals and applications. Chemical Industry Book Concern, Beijing, p 167
21. Bard AJ, Faulkner LR (2005) Electrochemical methods fundamentals and applications. Chemical Industry Book Concern, Beijing, pp 409–411
22. Bard AJ, Faulkner LR (2005) Electrochemical methods fundamentals and applications. Chemical Industry Book Concern, Beijing, p 163
23. Guo H, Tan Q (2000) Electrochemistry tutorial, 1st edn. Tianjin University Publishers, Tianjin, p 304
24. Miyazaki Y, Kajitani T (2001) J Cryst Growth 229:542
25. Wang WL, Wang YY, Wan CC (2006) J Electrochem Soc 153:C400
26. Heo P, Hagiwara K, Ichino R, Okido M (2006) J Electrochem Soc 153:C213
27. Cheaouni H, Bessieres J, Modaressi A, Heizmann JJ (2000) J Appl Electrochem 30:419